Delft University of Technology

Delft Center for Systems and Control

Technical report 17-011

Optimal power scheduling of fuel-cell-car-based microgrids*

I. Sarantis, F. Alavi, and B. De Schutter

If you want to cite this report, please use the following reference instead:

I. Sarantis, F. Alavi, and B. De Schutter, "Optimal power scheduling of fuel-cell-car-based microgrids," *Proceedings of the 56th IEEE Conference on Decision and Control*, Melbourne, Australia, pp. 5062–5067, Dec. 2017.

Delft Center for Systems and Control
Delft University of Technology
Mekelweg 2, 2628 CD Delft
The Netherlands
phone: +31-15-278.24.73 (secretary)
URL: `https://www.dcsc.tudelft.nl`

*This report can also be downloaded via `https://pub.deschutter.info/abs/17_011.html`

Optimal power scheduling of fuel-cell-car-based microgrids

Ioannis Sarantis, Farid Alavi, and Bart De Schutter

***Abstract*— A parking lot for fuel cell cars is considered inside a microgrid where the fuel cell cars are exploited to generate power inside the microgrid. A central control unit is considered in the microgrid in order to guarantee the power balance of the microgrid by means of scheduling the power generation of fuel cell cars. To compensate the uncertainty in the prediction of the load, three robust model predictive control methods are designed. Simulation of a case study compares the developed control methods and the performance of each method is evaluated.**

I. INTRODUCTION

The consequences of the uncontrolled and irresponsible use of fossil fuels, as well as the constantly rising CO_2 emissions around the globe require a turn towards more renewable ways of generating energy. An important step towards this direction is made by integrating renewable energy sources into power systems with the help of microgrids [1], [2]. Microgrids are structures that consist of loads and energy sources that provide energy and heat to their local area and they are treated as single controllable systems [3].

Fuel cell cars that are parked in a parking lot can be considered as the distributed generation units of a microgrid. The concept of fuel cell cars providing power to satisfy a load demand while being parked is called "Car as Power Plant" and is described analytically in [4]. Electricity, heat, and clean water are the products of the fuel cell cars and they can be used for commercial or industrial applications [5].

There are various examples in the literature where model predictive control (MPC) is used in order to optimally operate a microgrid. MPC is employed in [6] in order to control distributed renewable generation units that are integrated in an electrical grid. In [7], a supervisory model predictive controller is designed for optimal power management and control of a hydrogen-based microgrid. The authors of [8] use modeling techniques for hybrid systems in order to model the different components of the examined microgrid and to develop a model predictive controller that minimizes the microgrid's operational costs. The common disadvantage of all these MPC applications is that the inaccuracy in the prediction of the power demand that needs to be satisfied or the inaccuracy in the weather forecasts, when photovoltaic panels or wind turbines are used, is not taken into account when designing the controllers. The inherent uncertainty in the power demand prediction and in the power profile provided by the renewable generation units of a microgrid requires the use of robust MPC methods to guarantee the power balance condition.

The work in [9] uses robust MPC in order to control a microgrid that contains photovoltaic systems, wind turbines, and fuel cell electric vehicles. A min-max robust MPC approach is used to deal with the uncertainty of the power demand and of the renewable power generation. However, the control decisions are conservative as they are obtained by using the min-max method. Moreover, in [10], min-max robust MPC is employed to deal with the uncertainty in an islanded microgrid; however, in that paper, no exchange of power between the microgrid and the main power network is considered.

Chance-constrained robust MPC is employed in [11], where chance constraints are formed for the power exchange between the microgrid and the main power network in order to compensate for any power prediction uncertainty. In [11], the uncertainty is assumed to be normally distributed. In case of a constraint violation, the main power network provides the extra required power in order to ensure that the power balance is preserved inside the microgrid. However, the model of the microgrid does not include binary variables to represent the different modes of the power generation units and therefore, unaccepted scenarios like the simultaneous charging and discharging of the batteries could happen.

In [12], a scenario-based robust MPC technique is used for the optimal operation of a microgrid. In the formulation of the control method, the uncertainty due to fluctuating power demand and generation from renewable energy sources is taken into account and modeled by a finite number of scenarios. However, the problem setting in [12] minimizes the constraint violations in the cost function by using soft constraints without bounding the number of violations that occur.

In this paper, we consider the scenario of [13] and develop robust MPC methods for power scheduling of fuel cell cars. The main development of this paper compared to [13] is the development of three alternative robust MPC methods for the problem formulation. In addition, a simulation case study compares the developed methods to a standard min-max MPC algorithm.

The rest of this paper is organized as follows. Section II describes the modeling and the operational cost of the considered microgrid. In section III, we describe the developed robust MPC methods for power scheduling of the microgrid. A numerical case study shows the operation of the microgrid for all the developed methods in Section IV. Finally, Section V draws the main conclusions of this paper.

The authors are with the Delft Center for Systems and Control, Delft University of Technology, The Netherlands. f.alavi, b.deschutter @tudelft.nl

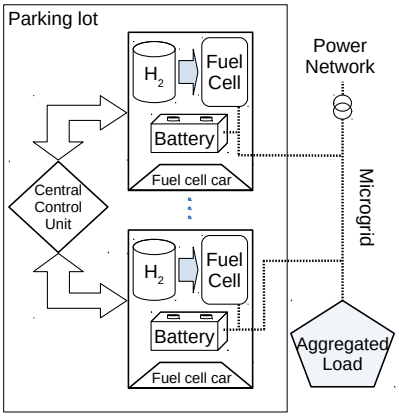

Fig. 1: Representation of the considered microgrid. The dashed lines indicate the electrical connections.

II. MODELING OF THE MICROGRID

A. Overview

The considered structure of the microgrid is the same as in [13] and is depicted in Figure 1. The microgrid can exchange power with the main power network. At the same time, the parking lot is able to generate electricity in order to cover the power demand of the load. If the aggregated load in addition to the power generation of the parking lot is positive, the excess power would be injected into the main power network. Conversely, the need for extra electricity inside the microgrid is compensated by draining power from the main power network. Considering the physical limitation of the power lines, there is a constraint on the maximum power exchange between the microgrid and the power network. We assume that the future load inside the microgrid is predictable with a reasonable accuracy. The difference between the predicted and the actual power demand is considered as an uncertainty in the system.

A central control unit is assumed inside the parking lot that can operate the fuel cells and the batteries of all parked cars. The objective of the controller is to operate the cars in such a way that, firstly, the physical constraints related to the operation of the cars and the maximum power exchange are satisfied and, secondly, the operational cost of the microgrid is minimized. Dealing with uncertainty in the prediction of the load requires a robust control algorithm for the central control unit; therefore, the objective of this paper is to develop chance-constrained and scenario-based robust MPC methods. The system is modeled in the simplest way because a simpler model results in the reduction of the computational burden of the robust MPC methods.

B. Fuel cell model

The fuel cell's behavior, while it is turned off and while it is turned on, is described in discrete time by the following piece-wise affine system [13], [14]:

$$x_{\mathrm{f},i}(k+1) = \begin{cases} x_{\mathrm{f},i}(k) & \text{if } s_{\mathrm{f},i}(k)=0 \\ x_{\mathrm{f},i}(k) - (\alpha_{\mathrm{f},i}u_{\mathrm{f},i}(k) + \beta_{\mathrm{f},i})T_{\mathrm{s}} & \text{if } s_{\mathrm{f},i}(k)=1, \end{cases} \quad (1)$$

where T_{s} is the sampling interval of the discrete-time system and $x_{\mathrm{f},i}(k)$ is the amount of hydrogen in the storage tank. Here, $\beta_{\mathrm{f},i}$ [$^{\mathrm{g}}/_{\mathrm{s}}$] is the rate with which the fuel cell consumes hydrogen in the stand-by operation mode, i.e. when the fuel cell is turned on but the net power generation is zero, and $\alpha_{\mathrm{f},i}$ [$^{\mathrm{g}}/_{\mathrm{J}}$] is the rate of hydrogen consumption due to the net power generation.

The continuous input $u_{\mathrm{f},i}(k)$ denotes the net power generation of the fuel cell i while the binary input $s_{\mathrm{f},i}(k)$ indicates the on $(s_{\mathrm{f},i}(k)=1)$ or off $(s_{\mathrm{f},i}(k)=0)$ operation mode of the fuel cell i. The definition of the input variables implies that:

$$u_{\mathrm{f},i}(k) > 0 \Leftrightarrow s_{\mathrm{f},i}(k) = 1. \quad (2)$$

If the minimum and the maximum power generation of the fuel cell are assumed to be zero and $\bar{P}_{\mathrm{f},i}$ respectively, then the continuous input $u_{\mathrm{f},i}(k)$ is bounded as:

$$0 \le u_{\mathrm{f},i}(k) \le \bar{P}_{\mathrm{f},i}. \quad (3)$$

C. Battery model

The battery of the fuel cell vehicle i can be charged at one time instant and discharged at another time instant. Therefore, two operation modes of the battery are needed in order to model it [8]. A continuous input $u_{\mathrm{b},i}(k)$ denotes the power that is exchanged between the battery and the microgrid. If the operation is in the charging mode, then $u_{\mathrm{b},i}(k)$ is positive; conversely, if the operation is in the discharging mode, then $u_{\mathrm{b},i}(k)$ is negative.

The energy stored in the battery is considered as the state of the battery, $x_{\mathrm{b},i}(k)$. As a result, the model of the battery is described by:

$$x_{\mathrm{b},i}(k+1) = \begin{cases} x_{\mathrm{b},i}(k) + \frac{T_{\mathrm{s}}}{\eta_{\mathrm{d},i}}u_{\mathrm{b},i}(k) & \text{if } s_{\mathrm{b},i}(k)=0 \\ x_{\mathrm{b},i}(k) + T_{\mathrm{s}}\eta_{\mathrm{c},i}u_{\mathrm{b},i}(k) & \text{if } s_{\mathrm{b},i}(k)=1, \end{cases} \quad (4)$$

where $s_{\mathrm{b},i}(k)$ is a binary variable indicating the charging $(s_{\mathrm{b},i}(k)=1)$ or discharging $(s_{\mathrm{b},i}(k)=0)$ operating mode. The charging and discharging efficiencies are $\eta_{\mathrm{c},i}$ and $\eta_{\mathrm{d},i}$, respectively. The definition of the input $u_{\mathrm{b},i}(k)$ and of the binary variable $s_{\mathrm{b},i}(k)$ implies that:

$$u_{\mathrm{b},i}(k) \ge 0 \Leftrightarrow s_{\mathrm{b},i}(k) = 1. \quad (5)$$

The physical limits on the maximum charging and discharging power of the battery imply that:

$$\underline{P}_{\mathrm{b},i} \le u_{\mathrm{b},i}(k) \le \bar{P}_{\mathrm{b},i}, \quad (6)$$

where $\underline{P}_{\mathrm{b},i}$ is the maximum power that can discharge the battery i and $\bar{P}_{\mathrm{b},i}$ is the maximum power that can charge the battery i.

D. Aggregated model of the microgrid

Taking into account the above models of the fuel cell and the battery, the state of vehicle i is defined as:

$$x_i(k+1) = x_i(k) + T_s \begin{bmatrix} -s_{f,i}(k)(\alpha_{f,i}u_{f,i}(k) + \beta_{f,i}) \\ s_{b,i}(k)(\eta_{c,i} - \frac{1}{\eta_{d,i}})u_{b,i}(k) + \frac{1}{\eta_{d,i}}u_{b,i}(k) \end{bmatrix}, \tag{7}$$

where $x_i(k) = [x_{f,i}(k), x_{b,i}(k)]^T$.

By defining $u_i(k) = [u_{f,i}(k), u_{b,i}(k), s_{f,i}(k)]^T$ and $z_i(k) = [z_{f,i}(k), z_{b,i}(k)]^T$, the state space model (7) can be transformed into the following mixed-logical dynamical form following the procedure of [15]:

$$x_i(k+1) = x_i(k) + b_{1,i}u_i(k) + b_{2,i}z_i(k) \tag{8}$$

where

$$b_{1,i} = \begin{bmatrix} 0 & 0 & -T_s\beta_{f,i} \\ 0 & \frac{T_s}{\eta_{d,i}} & 0 \end{bmatrix} \tag{9a}$$

$$b_{2,i} = \begin{bmatrix} -T_s\alpha_{f,i} & 0 \\ 0 & T_s(\eta_{c,i} - \frac{1}{\eta_{d,i}}) \end{bmatrix}. \tag{9b}$$

Considering the number of cars N_{veh} that are parked in the parking lot, the augmented state space model is defined as:

$$x(k+1) = x(k) + B_1u(k) + B_2z(k), \tag{10}$$

where $x(k) = \left[x_1^T(k), ..., x_{N_{veh}}^T(k)\right]^T$, $u(k) = \left[u_1^T(k), ..., u_{N_{veh}}^T(k)\right]^T$, and $z(k) = \left[z_1^T(k), ..., z_{N_{veh}}^T(k)\right]^T$. The matrices B_1 and B_2 are defined as

$$B_1 = \text{diag}\{b_{1,1}, ..., b_{1,N_{veh}}\} \tag{11a}$$

$$B_2 = \text{diag}\{b_{2,1}, ..., b_{2,N_{veh}}\}. \tag{11b}$$

The diag operator in (11a) and (11b), indicates that the matrices B_1 and B_2 are diagonal matrices, where the main diagonal is formed by the elements in the brackets.

E. Operational cost of the microgrid

The operational cost of the microgrid consists of several factors. Considering a prediction horizon N_p, the operational cost of the microgrid for the whole prediction period is defined as:

$$\begin{aligned} J(k) = \sum_{i=1}^{N_{veh}} \Bigg(& \sum_{k=0}^{N_p-1} \left(W_{f,i}|\Delta s_{f,i}(k)| - C_e(k)(u_{f,i}(k) - u_{b,i}(k))\right) \\ & + C_{H_2}\left(x_{f,i}(k) - x_{f,i}(k+N_p)\right) \\ & + C_{e,batt}\left(x_{b,i}(k) - x_{b,i}(k+N_p)\right)\Bigg) \\ & + \sum_{k=0}^{N_p-1} C_e(k)e_{in}(k). \end{aligned} \tag{12}$$

The operational cost of the system takes into account the consumption of hydrogen and the consumption of the energy that is stored in the batteries of the cars. The price of the hydrogen is denoted as C_{H_2} and the price of the energy of the batteries is denoted as $C_{e,batt}$. Moreover, $C_e(k)$ is the price of the electricity power and $e_{in}(k)$ is the power that is imported from the main power network at time step k.

The degradation cost is caused by the transition from one mode of the vehicle's fuel cell to another. For example, if the fuel cell is off and at the next time step it is switched on, this change of operational mode causes degradation. In (12), the Δ operator is used to represent the difference between two consecutive values of its operand, e.g. $\Delta s_{f,i}(k) = s_{f,i}(k) - s_{f,i}(k-1)$, and $W_{f,i}$ is a weight that is determined based on the specification of fuel cell i.

III. ROBUST MPC METHODS

A. Min-max robust MPC

The power balance inside the microgrid is described by the following power balance equation:

$$P_d(k) + \omega(k) = e_{in}(k) + \sum_{i=1}^{N_{veh}} \left(u_{f,i}(k) - u_{b,i}(k)\right), \tag{13}$$

where $P_d(k)$ is the prediction of the power demand of the load and $\sum_{i=1}^{N_{veh}} u_{f,i}(k) - u_{b,i}(k)$ is the power provided by the parking lot. The uncertainty, $\omega(k)$, in the system is unknown and denotes the deviation of the prediction of the power demand from its actual value.

The uncertainty $\omega(k)$ influences the operational cost of the microgrid through the power $e_{in}(k)$ that is exchanged with the main power network, which is assumed to be constrained as:

$$\underline{e}_{in} \leq e_{in}(k) \leq \bar{e}_{in}. \tag{14}$$

Therefore, the constraints that need to be satisfied regarding the power balance inside the microgrid read as:

$$P_d(k) + \omega(k) - \sum_{i=1}^{N_{veh}} \left(u_{f,i}(k) - u_{b,i}(k)\right) \geq \underline{e}_{in} \tag{15a}$$

$$P_d(k) + \omega(k) - \sum_{i=1}^{N_{veh}} \left(u_{f,i}(k) - u_{b,i}(k)\right) \leq \bar{e}_{in}. \tag{15b}$$

By assuming that the uncertainty is bounded such that:

$$\underline{\omega} \leq \omega(k) \leq \bar{\omega}, \tag{16}$$

a min-max robust MPC strategy for this problem setting is designed in [13]. The aim the proposed strategy is to minimize the operational cost of the microgrid with respect to the worst case realization of the uncertainty. The optimization problem of the min-max strategy in [13] is formulated as:

$$\begin{aligned} & \min_{\tilde{V}} \left\{\max\left\{W_0\tilde{V} + W_d\tilde{\bar{\omega}}, W_0\tilde{V} + W_d\tilde{\underline{\omega}}\right\}\right\} \\ & \text{subject to } A_1\tilde{V} \leq G_1. \end{aligned} \tag{17}$$

In (17), $\tilde{V}$ is the decision vector of the optimization problem over the prediction horizon, N_p, of MPC. Moreover, W_0 and W_d are constant matrices and $\tilde{\underline{\omega}} = [\underline{\omega}, \underline{\omega}, ..., \underline{\omega}]^T_{N_p \times 1}$ and $\tilde{\bar{\omega}} = [\bar{\omega}, \bar{\omega}, ..., \bar{\omega}]^T_{N_p \times 1}$. In addition, A_1 and G_1 are used in order to incorporate the power balance constraints (15) and the rest of the system's constraints, which are explicitly described in [13].

B. Chance-constrained robust MPC

In chance-constrained robust MPC the uncertainty is considered as a stochastic process. As a result, the cost function of the optimization problem depends on the expected value of the uncertainty. In this paper, the probability distribution of the uncertainty is assumed to be a truncated normal distribution, $\omega(k) \sim \mathrm{Tr}(0, \sigma^2, \underline{\omega}, \bar{\omega})$. Here, the mean of the assumed truncated distribution is zero, σ denotes the standard deviation of the distribution, and $\underline{\omega}$ and $\bar{\omega}$ represent the lower and the upper bound on the value of the random process respectively.

In general, in chance-constrained robust MPC we transform some, or all, of the system's constraints into probabilistic constraints. In this paper, we transform only the constraints (15) into probabilistic constraints as:

$$\Pr\left[\sum_{i=1}^{N_{\mathrm{veh}}}\left(u_{\mathrm{f},i}(k)-u_{\mathrm{b},i}(k)\right)-P_{\mathrm{d}}(k)-\omega(k)\leq -\underline{e}_{\mathrm{in}}(k)\right] \geq 1-\alpha \quad (18a)$$

$$\Pr\left[-\sum_{i=1}^{N_{\mathrm{veh}}}\left(u_{\mathrm{f},i}(k)-u_{\mathrm{b},i}(k)\right)+P_{\mathrm{d}}(k)+\omega(k)\leq \bar{e}_{\mathrm{in}}(k)\right] \geq 1-\alpha, \quad (18b)$$

where α is the probability level of the violation of the constraints. Therefore, by allowing the violation of the constraints in (15), any deviation of the load from the predicted values can be compensated by the main power network.

In general, the presence of a chance constraint inequality, such as (18), makes the optimization problem difficult to solve numerically because the constraints have a probabilistic form. However, by assuming that the distribution of the uncertainty in this case is approximated by the normal distribution, i.e. $\omega(k) \sim \mathrm{N}(0, \sigma^2)$, it is possible to use the inverse standard cumulative distribution function, Φ^{-1}, in order to obtain an easily solvable problem [11], [16]. Therefore, by using the inverse standard cumulative distribution function, the constraints (18) can be written as:

$$\sum_{i=1}^{N_{\mathrm{veh}}}\left(u_{\mathrm{f},i}(k)-u_{\mathrm{b},i}(k)\right)\leq -\underline{e}_{\mathrm{in}}(k)+P_{\mathrm{d}}(k)+\sigma\Phi^{-1}(1-\alpha) \quad (19a)$$

$$-\sum_{i=1}^{N_{\mathrm{veh}}}\left(u_{\mathrm{f},i}(k)-u_{\mathrm{b},i}(k)\right)\leq \bar{e}_{\mathrm{in}}(k)-P_{\mathrm{d}}(k)-\sigma\Phi^{-1}(1-\alpha). \quad (19b)$$

In chance-constrained robust MPC, the expected value of the uncertainty $\omega(k)$ appears in the cost function:

$$\min_{\tilde{V}} W_0\tilde{V}+W_{\mathrm{d}}\mathrm{E}[\tilde{\omega}], \quad (20)$$

where $\tilde{\omega}=[\omega(k),\omega(k+1),...,\omega(k+N_{\mathrm{p}}-1)]^{\mathrm{T}}$. Here, the stacked vector $\tilde{\omega}$ depends on k; however, k is dropped here and in the rest of this paper for the shake of simplicity. If the uncertainty has a normal distribution, i.e., $\omega(k) \sim \mathrm{N}(0, \sigma^2)$, then $E[\tilde{\omega}]=0$. Therefore, the optimization problem for the chance-constrained method reads as:

$$\min_{\tilde{V}} \; W_0\tilde{V} \quad \text{subject to } A_2\tilde{V}\leq G_2. \quad (21)$$

Here, A_2 and G_2 are used to express the constraints (19) and the rest of the system's constraints.

C. Standard scenario-based robust MPC

In the standard scenario-based robust MPC strategy, the uncertainty in the power demand prediction is assumed to be described by a finite number of scenarios: $\tilde{\omega}_s$ for $s=1,...,S$. We call a scenario as a sequence of uncertainties in consecutive time steps as $\tilde{\omega}_s=[\omega_s(k),\ldots,\omega_s(k+N_{\mathrm{p}}-1)]^{\mathrm{T}}$, where for all $j\in\{0,\ldots,N_{\mathrm{p}}-1\}$, $\omega_s(k+j)\in[\underline{\omega},\bar{\omega}]$. Each scenario $s=1,...,S$ is assigned to a probability of occurrence $p_s\in[0,1]$ and since the scenarios describe the same uncertainty it holds that:

$$\sum_{s=1}^{S} p_s = 1. \quad (22)$$

The standard scenario-based strategy uses the available scenarios that describe the uncertainty and aims to minimize the average operational cost of the microgrid, which depends on the available scenarios.

The constraints related to the limits of the exchanged power between the microgrid and the main power network are now defined as:

$$P_{\mathrm{d}}(k+j)+\omega_s(k+j)-\sum_{i=1}^{N_{\mathrm{veh}}}\left(u_{\mathrm{f},i}(k+j)-u_{\mathrm{b},i}(k+j)\right)\geq \underline{e}_{\mathrm{in}} \quad (23a)$$

$$P_{\mathrm{d}}(k+j)+\omega_s(k+j)-\sum_{i=1}^{N_{\mathrm{veh}}}\left(u_{\mathrm{f},i}(k+j)-u_{\mathrm{b},i}(k+j)\right)\leq \bar{e}_{\mathrm{in}}, \quad (23b)$$

which should hold for every scenario $s=1,...,S$.

Similar to the previous methods, in order to minimize the average operational cost, the following optimization problem should be solved:

$$\min_{\tilde{V}}\left\{W_0\tilde{V}+W_{\mathrm{d}}\sum_{s=1}^{S}p_s\tilde{\omega}_s\right\} \quad \text{subject to } A_3\tilde{V}\leq G_3. \quad (24)$$

D. Lenient-scenario-based robust MPC

The ability of the microgrid to exchange power with the main power network can be used to soften the constraints (23) that are related to the main power network limits. The soft constraints imply that this method is lenient on the violation of the constraints as now there is not any hard constraints related to the exchanged power with the main power network. Therefore, in this control strategy, the maximum capacity of power connection lines are not hard constraints, but a part of the cost in the optimization problem.

In order to soften the constraints, a penalty cost term is added to the cost function of the optimization problem (24). Therefore, the system cost function at time step k reads as:

$$W_0\tilde{V} + W_{\mathrm{d}} \sum_{s=1}^{S} p_s \tilde{\omega}_s + J_{\mathrm{p}}, \tag{25}$$

where J_{p} is a penalty term defined as:

$$\begin{aligned} J_{\mathrm{p}} = \sum_{s=1}^{S} \sum_{k=0}^{k+N_{\mathrm{p}}-1} C_{\mathrm{e}}(k) \max \Big\{ 0, \\ -P_{\mathrm{d}}(k) - \tilde{\omega}_{\mathrm{sub},s}(k) + \sum_{i=1}^{N_{\mathrm{veh}}} \big(u_{\mathrm{f},i}(k) - u_{\mathrm{b},i}(k)\big) + \underline{e}_{\mathrm{in}}, \\ P_{\mathrm{d}}(k) + \tilde{\omega}_{\mathrm{sub},s}(k) - \sum_{i=1}^{N_{\mathrm{veh}}} \big(u_{\mathrm{f},i}(k) - u_{\mathrm{b},i}(k)\big) - \bar{e}_{\mathrm{in}} \Big\}. \end{aligned} \tag{26}$$

If the constraint (23) is satisfied, then the penalty cost term is zero. Otherwise, a penalty term is added to the cost function that is equal to the amount of excess energy exchange between the microgrid and the power grid multiplied by the electricity price C_{e}.

In order to incorporate the cost function (25) in a Mixed Integer Linear Programming (MILP) problem, an auxiliary continuous variable, $c_s(k)$, is introduced that should satisfy the following constraints for all time steps k and for all of the scenarios:

$$c_s(k) \geq 0 \tag{27a}$$
$$c_s(k) \geq -P_{\mathrm{d}}(k) - \tilde{\omega}_s(k) + P_{\mathrm{vp}}(k) + \underline{e}_{\mathrm{in}} \tag{27b}$$
$$c_s(k) \geq P_{\mathrm{d}}(k) + \tilde{\omega}_s(k) - P_{\mathrm{vp}}(k) - \bar{e}_{\mathrm{in}}. \tag{27c}$$

In fact, the value of the auxiliary variable $c_s(k)$ indicates how much power is violating the main power network limits at time step k in the case that scenario s is realized.

By defining a new vector $\tilde{V}_2$ that includes both the previous optimization variables in $\tilde{V}$ and also the new auxiliary variables $\tilde{c}_s = [c_s(k), ..., c_s(k+N_{\mathrm{p}}-1)]^{\mathrm{T}}$, the optimization problem of the controller can be written as:

$$\begin{aligned} \min_{\tilde{V}_2} \Big\{ W_1\tilde{V}_2 + W_{\mathrm{d}} \sum_{s=1}^{S} p_s \tilde{\omega}_s \Big\} \\ \text{subject to } A_4\tilde{V}_2 \leq G_4, \end{aligned} \tag{28}$$

where W_1 is a constant matrix.

IV. CASE STUDY

The control strategies that were developed in Section III are now implemented in a case study where two fuel cell cars are considered inside the parking lot. The constant coefficients related to the fuel cells of the cars are assumed to be $\alpha_{\mathrm{f},1} = \alpha_{\mathrm{f},2} = \frac{0.47}{28} \cdot 10^{-3}$ [g/J] and $\beta_{\mathrm{f},1} = \beta_{\mathrm{f},2} = 0.03$ [g/s], based on the results of [14]. Moreover, the charging and discharging constants of the cars' batteries are assumed to be $\eta_{\mathrm{c},1} = \eta_{\mathrm{d},1} = 0.9$ and $\eta_{\mathrm{c},2} = \eta_{\mathrm{d},2} = 0.8$ respectively, according to [17].

The owners of the fuel cell cars require that the amount of hydrogen in the storage tank does not become less than 1 kg and the energy that is stored in each battery is required to remain between 10 kWh and 24 kWh.

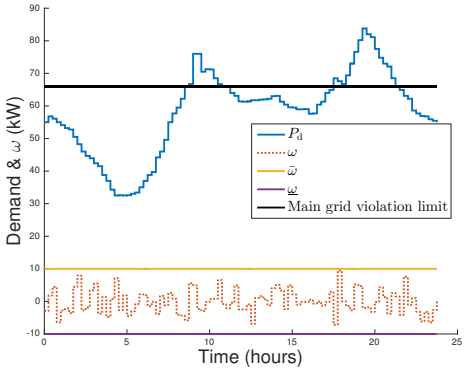

Fig. 2: Power demand, P_{d}, that needs to be satisfied in 24 hours and uncertainty ω

Furthermore, the maximum power generation of each fuel cell is assumed to be 30 kW. The maximum power of charging or discharging the batteries is assumed to be 2 kW. In addition, we assume a connection between the microgrid and the power grid with a maximum power exchange capability of 66 kW. Therefore, the exchanged power between the microgrid and the main power network is constrained to be in the interval [-66, 66] kW.

The probability level of the violation of the constraints for the chance-constrained robust MPC method is set to $\alpha = 0.05$. The scenarios of the uncertainty for the scenario-based methods and the realized uncertainty follow the truncated normal distribution, i.e. $\mathrm{Tr}(0, \sigma^2, \underline{\omega}, \bar{\omega})$. Here, $\sigma = \frac{\max\{|\bar{\omega}|, |\underline{\omega}|\}}{3}$.

The 24-hours predicted power demand that needs to be satisfied is adapted from [13] and is depicted in Figure 2. Moreover, this figure shows the bounds of the considered uncertainty in the power demand, which are $\underline{\omega} = -10$ kW and $\bar{\omega} = 10$ kW, as well as the realized uncertainty, ω. A scenario set that contains 50 scenarios of the uncertainty is considered for the scenario-based methods and all the scenarios that belong to the scenario set are considered to be equiprobable.

The simulation is performed in MATLAB R2015b [18] and the solver Gurobi [19] is used in order to solve the MILP problem of each method.

The three new developed robust MPC methods are able to provide a less conservative power scheduling of the microgrid compared to the min-max strategy, as it is depicted in Table I. This table provides a comparison between the operational closed-loop cost of the microgrid, the number of the constraint violations, and the violating power for each method in 24 hours. Furthermore, the power that is imported from the main power network in the chance-constrained and the lenient-scenario-based methods is depicted in Figure 3. Any value of imported power above the black line in this figure shows a violation of the main power network constraints.

All the new developed methods reduce the operational cost

TABLE I: Operational closed-loop cost (€), number of constraint violations, total violating power (kW), and peak of violating power (kW)

	Min-max	Chance-constrained	Standard scenario-based	Lenient-scenario-based
Operational closed-loop cost (€)	245.83	217.97	228.41	215.06
Number of constraint violations	0	4	1	7
Total violating power (kW)	0	7.22	3.54	12.47
Peak of violating power (kW)	0	3.97	3.54	4.31

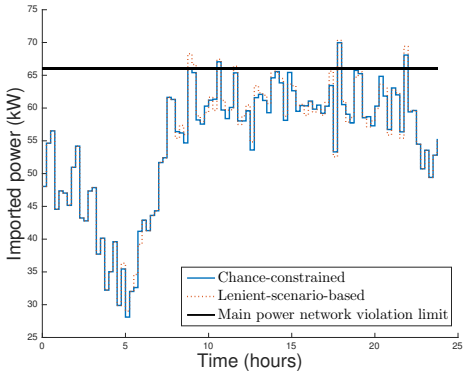

Fig. 3: Imported power from the main power network related to the chance-constrained method and the lenient-scenario-based method

of the microgrid. The most violations happen in the lenient-scenario-based method because of the soft constraints. In addition, the standard scenario-based strategy cannot guarantee the satisfaction of the power exchange constraint, as one violation has happened in our simulation. The peak of the violating power in all of the developed methods is relatively small considering the bounds of the uncertainty, which implies that the main power network is not continuously strained by the violating power.

If the violation of the main power network constraints does not result in a critical situation, which we have assumed for typical power connection lines between a microgrid and the power network, the lenient-scenario-based robust MPC strategy results in lower operational costs compared to the other developed methods. However, a chance-constrained method allow us to set a bound on the constraints violation, and, hence, this method can control the strain on the power connection lines.

V. CONCLUSIONS

In this paper, we have developed three robust MPC strategies for the optimal power scheduling of the fuel-cell-car-based microgrid; namely, the chance-constrained, the scenario-based, and the lenient-scenario-based method. An advantage of the methods developed in this paper compared to the min-max approach developed in [13] is the reduction of conservatism and reaching a better system performance. The improvement in the system performance is achieved at the cost of violating constraints. Among the three developed control methods, the chance-constrained method allows us to determine the probability of the constraint violations. The lenient-scenario-based method results in a satisfactory low operational cost compared to the standard scenario-based method. However, the standard scenario-based method has a lower rate of constraint violations compared to the lenient scenario-based method. The severity of the constraint violations in real applications is the key in the selection of the most suitable control method.

VI. ACKNOWLEDGMENTS

This research is supported by the NWO-URSES project Car as Power Plant, which is financed by the Netherlands Organization for Scientific Research (NWO).

REFERENCES

[1] N. Hatziargyriou, H. Asano, R. Iravani, and C. Marnay, "Microgrids," *IEEE Power and Energy Magazine*, vol. 5, no. 4, pp. 78–94, 2007.
[2] H. Farhangi, "The path of the smart grid," *IEEE Power and Energy Magazine*, vol. 8, no. 1, pp. 18–28, 2010.
[3] R. H. Lasseter, "MicroGrids," in *Power Engineering Society Winter Meeting*, pp. 305–308, 2002.
[4] A. van Wijk and L. Verhoef, *Our Car as Power Plant*. IOS Press BV, 2014.
[5] A. Fernandes, T. Woudstra, A. van Wijk, L. Verhoef, and P. V. Aravind, "Fuel cell electric vehicle as a power plant and SOFC as a natural gas reformer: An exergy analysis of different system designs," *Applied Energy*, vol. 173, pp. 13–28, 2016.
[6] W. Qi, J. Liu, and P. D. Christofides, "A distributed control framework for smart grid development: Energy/water system optimal operation and electric grid integration," *Journal of Process Control*, vol. 21, no. 10, pp. 1504–1516, 2011.
[7] L. Valverde, C. Bordons, and F. Rosa, "Power management using model predictive control in a hydrogen-based microgrid," *IECON 2012 - 38th Annual Conference on IEEE Industrial Electronics Society*, pp. 5669–5676, 2012.
[8] A. Parisio, E. Rikos, G. Tzamalis, and L. Glielmo, "Use of model predictive control for experimental microgrid optimization," *Applied Energy*, vol. 115, pp. 37–46, 2014.
[9] F. Alavi, E. Park Lee, N. van de Wouw, B. De Schutter, and Z. Lukszo, "Fuel cell cars in a microgrid for synergies between hydrogen and electricity networks," *Applied Energy*, vol. 192, pp. 296–304, 2017.
[10] C. A. Hans, V. Nenchev, J. Raisch, and C. Reincke-Collon, "Minimax model predictive operation control of microgrids," in *Proceedings of the 19th IFAC World Congress*, pp. 10287–10292, 2014.
[11] M. Gulin, J. Matusko, and M. Vasak, "Stochastic model predictive control for optimal economic operation of a residential DC microgrid," *IEEE International Conference on Industrial Technology (ICIT)*, pp. 505–510, 2015.
[12] A. Parisio, E. Rikos, and L. Glielmo, "Stochastic model predictive control for economic/environmental operation management of microgrids: An experimental case study," *Journal of Process Control*, vol. 43, pp. 24–37, 2016.
[13] F. Alavi, N. V. D. Wouw, and B. D. Schutter, "Min-Max Control of Fuel-Cell-Car-Based Smart Energy Systems," in *2016 European Control Conference*, pp. 1223–1228, 2016.
[14] P. Rodatz, G. Paganelli, A. Sciarretta, and L. Guzzella, "Optimal power management of an experimental fuel cell/supercapacitor-powered hybrid vehicle," *Control Engineering Practice*, vol. 13, no. 1, pp. 41–53, 2005.
[15] A. Bemporad and M. Morari, "Control of systems integrating logic, dynamics, and constraints," *Automatica*, vol. 35, no. 3, pp. 407–427, 1999.
[16] A. T. Schwarm and M. Nikolaou, "Chance-constrained model predictive control," *AIChE Journal*, vol. 45, no. 8, pp. 1743–1752, 1999.
[17] A. Parisio, E. Rikos, and L. Glielmo, "A model predictive control approach to microgrid operation optimization," *IEEE Transactions on Control Systems Technology*, vol. 22, no. 5, pp. 1813–1827, 2014.
[18] MATLAB–MathWorks. `https://www.mathworks.com/product/matlab.html`.
[19] Gurobi optimization. `http://www.gurobi.com`.